

# Analyzing Age of Information in Prioritized Status Update Systems using Probabilistic Hybrid Discipline

Tamer E. Fahim<sup>1,3</sup>, Sherif I. Rabia<sup>1,3</sup>, Ahmed H. Abd El-Malek<sup>2</sup> and Waheed K. Zahra<sup>1,4</sup>

<sup>1</sup>Basic and Applied Sciences Institute, Egypt-Japan University of Science and Technology, Alexandria, Egypt

<sup>2</sup>School of Electronics, Communications and Computer Engineering, Egypt-Japan University of Science and Technology, Alexandria, Egypt

<sup>3</sup>Department of Engineering Mathematics and Physics, Faculty of Engineering, Alexandria University, Alexandria, Egypt

<sup>4</sup>Department of Engineering Physics and Mathematics, Faculty of Engineering, Tanta University, Tanta, Egypt

**Keywords:** Age of Information, Queuing Models, Stochastic Hybrid Systems, Internet of Things.

**Abstract:** The ubiquitous deployment of the internet of things technology engenders great attention to the real-time status update systems. However, the real-life situation implies the service differentiation between sources according to their sensitivity, a problem that is rarely addressed in the literature. This situation is to be handled classically by adopting the preemption or non-preemption service disciplines. In any of these disciplines, an improvement is yielded for some specific classes with a severe degradation for the others. To address this paradox, we propose a probabilistic hybrid service discipline, by which the decision of preemption for each class is controlled by a probabilistic parameter. The stochastic hybrid system approach is employed to analyze the average age of information for each class. A numerical study of a three-class prioritized network demonstrates the significance of the proposed model to compromise the performance of all classes even in the worse traffic loading conditions. Moreover, three different approaches are proposed to adjust the probabilistic hybrid parameters for more promising results.

## 1 INTRODUCTION

Recently, the unprecedented growth in wireless communication networks and portable devices has raised the importance of real-time status update systems (Yates et al., 2021). In such systems, the transmitting node incorporating a sensor is responsible for tracking the physical phenomenon of interest before sending its status updates to a remote interested recipient (Kaul et al., 2012a).

Lately, the status update system has been widely deployed in a myriad of real-life applications, such as autonomous vehicular network (Talak et al., 2016), Health-care monitoring system (Mishra et al., 2020) and smart manufacturing system (Xu and Gautam, 2020), to name a few. In such applications, status update packets, unlike conventional data packets, lose their value and importance after being aged (Sun

et al., 2017). Accordingly, the freshness is an important criterion of real-time status update system to guarantee reliable control and monitoring. However, the objective to enhance the information freshness is different from the problem of maximizing the throughput or minimizing the delay (Abbas et al., 2021). To illustrate, enhancing the system throughput, by increasing the transmission rate, deteriorates information freshness due packets backlogging. On the other hand, sending status updates with lower update rates ensures minimum-delay transmission, while degrading information freshness due to packet obsolescence.

Accordingly, a new performance measure has been introduced (Kaul et al., 2012a), conforming with the notion of information freshness, called as age of information (AoI)  $\Delta(t)$ . It is defined as the ongoing time since the generation of the latest received update packet (Costa et al., 2016),  $\Delta(t) = t - u(t)$ , where  $u(t)$  is the generation time of the freshest packet received at the monitor.

The mathematical framework of the AoI is firstly introduced in (Kaul et al., 2012a), where the average

<sup>a</sup>  <https://orcid.org/0000-0002-9293-1202>

<sup>b</sup>  <https://orcid.org/0000-0003-1471-8841>

<sup>c</sup>  <https://orcid.org/0000-0002-7906-815X>

<sup>d</sup>  <https://orcid.org/0000-0002-6448-6877>

AoI of a single-source stream has been analyzed using some simple queueing abstractions,  $M/M/1$ ,  $M/D/1$  and  $D/M/1$ . The First Come First Served (FCFS) queueing policy has been deployed to manage the access of the update packets to the server. However, in (Kaul et al., 2012b), two variations of the Last Come First Served (LCFS) have been addressed:  $M/M/1/1$  with preemption service (PR-S) and  $M/M/1/2^*$ . In the former the ongoing service can be interrupted from the newly arrived packet, while the latter admits the preemption only on a waiting position of size 1 (PR-W policy).

Similar to the case of the single-source stream, the case of multi-source stream engenders a host of research work. In (Yates and Kaul, 2018), the lossless system modelled as  $M/M/1$  with FCFS is compared with two models of the lossy system,  $M/M/1/1$  with PR-S and  $M/M/1/2^*$ . In this work, the stochastic hybrid system (SHS) approach is used for the first time to analyze the average AoI. Furthermore, according to (Farazi et al., 2019), the  $M/M/1/1$  with self-preemption (SP) has been addressed, where the preemption is admitted only between the packets belonging to the same source.

Most of the research work pertaining to the case of multi-source stream assume the same service treatment for all streams irrespective of their belonging source. However, the more practical situation implies the service differentiation between sources' streams according to some criteria. For instance, in the vehicular network, safety-centric updates are more age sensitives compared with other regular updates (Maatouk et al., 2019). Such interesting case has been rarely addressed in the context of the age of information. In (Kaul and Yates, 2018), the author extends his work in (Yates and Kaul, 2018) to be deployed under the prioritized case. However, in (Najm et al., 2019), two prioritized streams are considered. The  $M/G/1/1$  with PR-S is adopted for the highest class, while two cases are experimented for the lowest class,  $M/G/1/1$  with PR-S and  $M/G/1$  with FCFS. It is then proved that  $M/M/1/1$  with PR-S is no longer the optimal for a certain class under the existence of a higher priority one. Subsequently, in (Maatouk et al., 2019), separate queue of size 1 is considered for each priority class, instead of assigning one waiting position for all classes (Kaul and Yates, 2018). This is to store the preempted packet, where the preemption is applied over both the packet being queued and at the packet being served. However, the traffic parameter setting is limited to be identical within all classes under the exponential service time distribution. This limitation has been abandoned afterwards in (Xu and Gautam, 2020) by considering heterogeneous traffic with gen-

eral service time distribution. In this study, the Peak age of information, which is an alternative measure of the AoI (Costa et al., 2016), has been examined. The non-preemption (NP) service discipline is assumed, where the ongoing service is guarded from any interruptions.

In the aforementioned research work (Kaul and Yates, 2018; Najm et al., 2019; Maatouk et al., 2019; Xu and Gautam, 2020), the prioritized streams are handled in the server whether in preemptible or non-preemptible basis. Each one of these schemes significantly improves the performance of some particular class at the cost of a dramatic degradation of the others (Kim, 2012).

This paradox can be resolved using the notion of hybrid preemption/non-preemption service discipline (Fahim et al., 2018). In this discipline, the decision whether to preempt the ongoing service or not is governed by a discretionary rule employed at the server. There are four distinct approaches of this rule, mentioned in the literature of the priority queueing system (Kim, 2012). However, the hybrid service discipline has not been addressed so far in the AoI context.

Based on the foregoing, we propose a probabilistic hybrid service discipline under the prioritized  $M/M/1/1$  queueing abstraction. In such case, the decision of preemption for class  $m$  is taken with probability  $p_m$ . The AoI for each prioritized class is then modelled and analyzed using SHS approach, by which the average AoI for each class is obtained. After that a numerical study of three prioritized classes is conducted. The performance of our proposed model is compared with the priority preemption (PP) model mentioned in (Kaul and Yates, 2018), along with the SP model mentioned in (Farazi et al., 2019) while taking into consideration the priority setting. The numerical results demonstrate that the proposed hybrid discipline significantly reduces the downside effect caused by the PP and SP models, more specifically at the worse traffic loading conditions. It is also shown that the probabilistic parameters  $p_m$  can be adjusted to optimize a cost function, which represents the level of satisfaction of the whole network. Furthermore, the design of the admission control policy reflects the superiority of our proposed model, where the admission region becomes more wider over the whole span of the traffic loading condition.

The rest of this paper is organized as follows. In Section 2, the system model is described with the related assumptions in addition to the declaration of the corresponding traffic parameters. Subsequently, Section 3 presents the AoI analysis of the proposed model with a brief preliminary on the SHS approach. After that, the numerical results and investigations are pre-

sented in Section 4. Finally, our conclusion and future work are summarized in Section 5.

## 2 SYSTEM MODEL

### 2.1 System Description and Assumptions

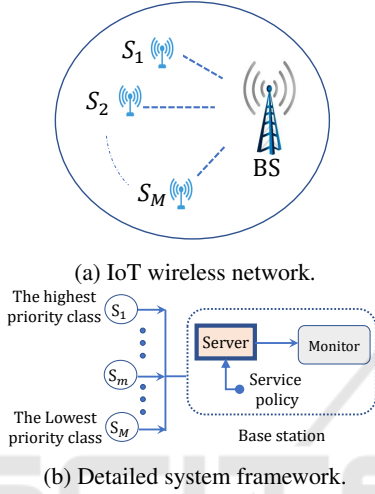


Figure 1: Considered system model's description.

In our work, a typical wireless internet of things (IoT) network is considered as shown in Figure 1a. It consists of  $M$  IoT sources  $S_m$  ( $1 \leq m \leq M$ ) and one centralized base station (BS) as a receiving node. Following the distinction in the AoI constraints between sources, the IoT sources are prioritized such that class  $m$  has a higher priority over class  $n$ , subject to  $1 \leq m \leq n \leq M$ .

The detailed system framework of the aforementioned IoT network is illustrated as shown in Figure 1b. As shown, there is no buffer to store source packets. Moreover, in the receiving end, the multiple-access request of the priority classes is scheduled according to the priority order. To illustrate,  $S_m$  has a higher priority to access the server over  $S_n$ , for  $m < n$ . After the scheduling process, the selected packet that has the turn is to be processed through the server, which is governed by a service policy.

*service policy.* It governs the interaction between the source being served and the source requesting the service. In our proposed scheme, the service policy has the following features: Firstly, the self-preemptions are admitted, where a packet being served can be replaced by a freshest one that belongs to the same source. Secondly, while serving the higher priority class, any packet request from

the lower priority class is declined and dropped from the system. Thirdly, the probabilistic hybrid (PR/NP) scheme is proposed, where class  $m$  being served can be preempted from the higher priority classes with probability  $p_m$ , before being dropped from the system. Accordingly, this proposed scheme will be referred to as probabilistic hybrid service discipline, where each priority class, except class 1, has its own probabilistic parameter  $0 \leq p_m \leq 1$ , for  $2 \leq m \leq M$ . Moreover, it should be noted that if  $p_m = 1$  for  $1 \leq m \leq M$ , the probabilistic hybrid discipline reduces to the PP model (Kaul and Yates, 2018). On the other hand, if  $p_m = 0$  for  $1 \leq m \leq M$ , the hybrid approach reduces to the self-preemption (SP) model, which is similar to the model in (Farazi et al., 2019) but with considering the priority setting.

### 2.2 Traffic Parameters

Regarding the analytical framework, an  $M/M/1/1$  priority queueing system is proposed. The Poisson process is assumed to capture the arrival process of the status update stream of each priority class, with an arrival rate  $\lambda_m$ , for  $1 \leq m \leq M$ . In this regards, let  $\hat{\lambda}_m = \sum_{i=1}^{m-1} \lambda_i$  and  $\check{\lambda}_m = \sum_{i=m+1}^M \lambda_i$  denote the aggregate arrival rate of the higher and the lower priority classes of class  $m$ , respectively. Hence,  $\lambda_{\text{total}} = \hat{\lambda}_m + \lambda_m + \check{\lambda}_m$ . The processing time of each priority class is assumed to follow the exponential distribution, with service rate  $\mu_m$ , for  $1 \leq m \leq M$ . In the subsequent analytical work, it is assumed that all classes has the same processing requirements, hence; we can suppress the class notation as  $\mu_m = \mu$ . Accordingly, let's also denote  $S_m$  offered load as  $\rho_m = \frac{\lambda_m}{\mu}$ ; hence,  $\hat{\rho}_m = \frac{\hat{\lambda}_m}{\mu}$  and  $\check{\rho}_m = \frac{\check{\lambda}_m}{\mu}$ . Consequently, the total offered load by all classes is  $\rho_{\text{total}} = \hat{\rho}_m + \rho_m + \check{\rho}_m$ .

## 3 PERFORMANCE ANALYSIS

In our analytical framework, the main target is to evaluate the average age of information for each priority class ( $E[\Delta_m]$ ,  $1 \leq m \leq M$ ). In this regard, the SHS approach is deployed, which is guaranteed to be more tractable approach in case of finite-state system (Yates and Kaul, 2018). Accordingly, a brief preliminary on the AoI-related SHS approach will be firstly presented in Section 3.1. After that, Section 3.2 will present the SHS analysis related to the proposed prioritized  $M/M/1/1$  queueing model under the probabilistic hybrid service discipline.

### 3.1 Preliminary on the AoI-Related SHS

The SHS is generally defined as a stochastic system with random dynamics, where its states are a hybrid of discrete component  $q(t)$  and continuous component  $\mathbf{x}(t)$ . The discrete component  $q(t) \in \mathcal{Q} = \{0, 1, \dots, m\}$  represents the evolution of the system occupancy upon the occurrence of some stochastic events (e.g. packet arrival and departure events). On the other hand, the continuous component  $\mathbf{x}(t) = [x_0(t), \dots, x_n(t)] \in \mathbb{R}^{(n+1)}$  describes a continuous-time tracking of  $n+1$  AoI-related processes, where  $n$  is the system capacity of packets. Here,  $x_0(t)$  is the AoI process at the monitor (after packet departure); however,  $x_i$  for  $1 \leq i \leq n$  are the AoI tracking of each packet being trapped in the system. In the subsequent context, the main idea of the AoI-related SHS is summarized.

Firstly, as our focus is placed on the system with memoryless service process, the discrete component  $q(t) \in \mathcal{Q}$  can be modeled as a Continuous-time Markov chain (CTMC) denoted as  $(\mathcal{Q}, L)$ , where  $L$  is the set containing all transitions between the discrete nodes  $\mathcal{Q}$ . To illustrate, the transition  $l \in L$  is a directed path from node  $q_l$  to  $q'_l$  with a transition rate  $\lambda^{(l)} \delta_{q_l, q'_l}$ . The Kronecker delta function is used here so that this transition rate is strictly related to the occurrence of  $q(t) = q_l$ . Moreover, let's define  $L'_q = \{l \in L : q'_l = q\}$  and  $L_q = \{l \in L : q_l = q\}$  to be the corresponding sets of the entering and departing transitions of node  $q$ .

Regarding the continuous-time evolution of the component  $\mathbf{x}(t)$ , it will be in two directions: the evolution upon each transition  $l$  and the evolution while being trapped at each node  $q$ . In the former, a linear reset mapping occurs upon each transition  $l$ . In simple words, at each transition  $l$ , the discrete state changes from  $q_l$  to  $q'_l$ ; meanwhile, the continuous state resets from  $\mathbf{x}$  to  $\mathbf{x}' = \mathbf{x} \mathbf{A}_l$ . The matrix  $\mathbf{A}_l$  is called the reset maps of transition  $l$ . However, the AoI context implies that the matrix  $\mathbf{A}_l$  should be with binary entries,  $\mathbf{A}_l \in \{0, 1\}^{(n+1) \times (n+1)}$ . When it comes to the evolution of  $\mathbf{x}$  at each node, there are a lot of SHS variation in this regard (Teel et al., 2014). However, in the AoI context, the piecewise linear SHS variation is deployed (Hespanha, 2006). In such case, the evolution of  $\mathbf{x}(t)$  at each node  $q$  is  $\dot{\mathbf{x}} = \mathbf{b}_q$ , where  $\mathbf{b}_q \in \{0, 1\}^{1 \times (n+1)}$  is a vector with binary elements. To illustrate, The entry  $b_q^k = 1$  means that the  $x_k$  increases linearly with time while being at state  $q$ ; however, the entry  $b_q^k = 0$  indicates a plateau in  $x_k$  in its previous value. Moreover, the entry  $b_q^k$  is assumed to be 0 if  $x_k$  is irrelevant at state  $q$ , i.e. there is no need

to be tracked at state  $q$ .

Based on the foregoing, the AoI analysis using SHS begins with defining the following quantities for each node  $q$ :

$$\pi_q(t) = \mathbb{E}[\delta_{q,q(t)}], \quad (1)$$

$$v_{q,j}(t) = \mathbb{E}[x_j(t) \delta_{q,q(t)}], \quad 0 \leq j \leq n, \quad (2)$$

and the corresponding vector function

$$\mathbf{v}_q(t) = [v_{q,0}(t), \dots, v_{q,n}(t)] = \mathbb{E}[\mathbf{x}(t) \delta_{q,q(t)}]. \quad (3)$$

Here,  $\pi_q(t)$  represents the state probabilities ( $\pi_q(t) = \mathbb{P}[q(t) = q]$ ). However, the vector  $\mathbf{v}_q(t)$  symbolizes the correlation vector between  $\mathbf{x}(t)$  and the discrete state  $q$ . In other words, it represents the corresponding average values of the AoI-related processes while being at state  $q$ .

The AoI analysis starts by finding the state probability at each state  $q$  ( $\pi_q(t)$ ). However, a basic assumption in this regard is that the CTMC of  $q(t)$  is ergodic. In such case, the state probabilities  $\pi_q(t)$  converges to a certain limit  $\bar{\pi}_q$  according to the following system of linear equations:

$$\bar{\pi}_q \left( \sum_{l \in L_q} \lambda^{(l)} \right) = \sum_{l \in L'_q} \lambda^{(l)} \bar{\pi}_{q_l}, \quad q \in \mathcal{Q}, \quad (4)$$

$$\sum_{q \in \mathcal{Q}} \bar{\pi}_q = 1. \quad (5)$$

After solving the system described by (4) and (5), the stationary probability vector is yielded,  $\bar{\pi} = [\bar{\pi}_0, \dots, \bar{\pi}_m]$ . Regarding the correlation vector  $\mathbf{v}_q(t)$ , as declared in (Yates and Kaul, 2018), it satisfies the following first order differential equations, for all  $q \in \mathcal{Q}$ :

$$\dot{\mathbf{v}}_q(t) = \mathbf{b}_q \pi_q + \sum_{l \in L'_q} \lambda^{(l)} \mathbf{v}_{q_l}(t) \mathbf{A}_l - v_q(t) \left( \sum_{l \in L_q} \lambda^{(l)} \right). \quad (6)$$

The stability issue of this system of differential equations is addressed in (Yates and Kaul, 2018). It is proved that the stability of this system depends on the reset maps matrix  $\mathbf{A}_l$ . In case of being a stable system,  $\dot{\mathbf{v}}_q(t) = 0$  and the resulting  $\mathbf{v}_q(t)$  converges to a certain limit  $\bar{\mathbf{v}}_q$  as  $t \rightarrow \infty$ . In such case the system of differential equations is reduced to a system of linear equations as follows:

$$\bar{\mathbf{v}}_q \left( \sum_{l \in L_q} \lambda^{(l)} \right) = \mathbf{b}_q \pi_q + \sum_{l \in L'_q} \lambda^{(l)} \bar{\mathbf{v}}_{q_l} \mathbf{A}_l, \quad q \in \mathcal{Q}. \quad (7)$$

In this regard, it is proved by Theorem 4 of (Yates and Kaul, 2018) that the stability of the system (6) can be guaranteed if the system (7) yields a non-negative solution  $\bar{\mathbf{v}} = [\bar{\mathbf{v}}_0, \dots, \bar{\mathbf{v}}_m]$ . Consequently, the average AoI at the monitor  $\mathbb{E}[\Delta]$  can be evaluated from the corresponding AoI-related process  $\mathbb{E}[x_0]$ , which can be

evaluated as follows:

$$\begin{aligned} E[x_0] &= \lim_{t \rightarrow \infty} E[x_0(t)] = \lim_{t \rightarrow \infty} \sum_{q \in Q} E[x_0(t) \delta_{q,q(t)}] \\ &= \sum_{q \in Q} v_{q,0}. \end{aligned} \quad (8)$$

Hence,

$$E[\Delta] = \sum_{q \in Q} v_{q,0}. \quad (9)$$

### 3.2 The Probabilistic Hybrid Service Discipline: SHS Analysis

In this section, the foregoing SHS definitions and analysis will be applied under the proposed model described in 2. In this study, the aim is to study the age of information of the priority class of interest  $m$  out of  $M$  prioritized classes. Accordingly, the subsequent analytical framework is perceived from the perspective of class  $m$ .

Under the proposed scheme, the discrete states characterization will be  $q(t) \in Q = \{0, \text{HP}, m, m+1, \dots, m+i, \dots, M\}$  for  $1 \leq i \leq M-m$ . Here, state 0 represents that the server is in the idle case, and state  $m$  denotes that the class of interest  $S_m$  is being served. However, state HP means that the ongoing service belongs to any higher priority class than class  $m$  regardless of its priority index. This is because any of them have the same effect from class  $m$  perspective, the preemption with probability  $p_m$ . On the other hand, the remaining states of  $Q$  symbolize all lower priority classes than class  $m$ . Let denote LP =  $\{m+1, \dots, m+i, \dots, M\}$  for  $1 \leq i \leq M-m$ . In contrast with the state HP, all lower priority classes should be included in the discrete state notation of the SHS. This is due to the distinction of the probabilistic hybrid parameters  $p_m$ . Accordingly, for presentation convenience, state  $m+i$  ( $1 \leq i \leq M-m$ ) is a representative state for all lower priority classes in state LP.

On the other side of the problem, since the system is bufferless, the continuous state is defined as  $\mathbf{x}(t) = [x_0(t), x_1(t)]$ , where  $x_0(t)$  and  $x_1(t)$  are the AoI related processes of class  $m$  at the monitor and the server, respectively. It should be noted that  $x_1(t)$  measures the time span from the time class  $m$  starts the service until being departed whether due to service completion or service preemption. However,  $x_0(t)$  will be reset to  $x_1(t)$  in the case of service completion only. On the other hand, the evolution of the AoI-related processes  $\mathbf{x}(t)$ , while being trapped at discrete state  $q \in Q$ , is formulated as the following differential equation.

$$\dot{\mathbf{x}}(t) = b_q = \begin{cases} [1 & 1], & q = m \\ [1 & 0], & q \in Q \setminus m \end{cases}. \quad (10)$$

To illustrate, the AoI process  $x_0(t)$  increase with a unit rate while being trapped at each discrete state before any transition. However,  $x_1(t)$  increase linearly only if class  $m$  is being served, while the other states are irrelevant to class  $m$ .

Our goal is to evaluate the correlation vector  $\bar{\mathbf{v}}_q = [\bar{v}_{q0}, \bar{v}_{q1}]$  for each  $q \in Q$  by solving the system of linear equations, described in (7), so that we can evaluate average AoI  $E[\Delta_m]$  using (9). To do that, Figure 2 illustrates the resulting SHS Markov chain (MC) as perceived by the class of interest  $m$ . As shown, state  $m+i$  ( $1 \leq i \leq M-m$ ) is a combined state for all lower priority classes considered in state LP. Moreover, Table 1 elaborates all state transitions ( $l$ ) related to the relevant class  $m$  and other irrelevant classes. As shown, all transition rates ( $\lambda^{(l)}$ ) and the corresponding reset maps ( $\mathbf{A}_l$ ) are tabulated, along with  $\mathbf{v}_{q_l} \mathbf{A}_l$  that will be used in (7). It is noted that all state transitions are classified into four blocks, with some categories for each one.

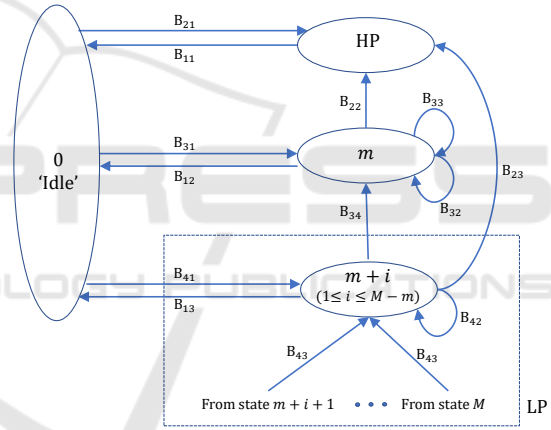


Figure 2: The SHS MC for class  $m$  under the proposed scheme.

According to Figure 2 and Table 1, the explanation of each transition  $l$  is discussed as follows:

- B1: The transitions in this block are related to the departure epochs of the packet being served. In all categories related to this block, the new state  $q'_l = 0$  is irrelevant to class  $m$ ; hence,  $x'_1 = 0$ . Moreover, in categories  $B_{11}$  and  $B_{13}$ , the departing packet is not related to class  $m$ , therefore, there is no change in  $x_0$  ( $x'_0 = x_0$ ). In contrast, in  $B_{12}$ , the departing class  $m$  resets the signal  $x_0$  to  $x_1$ , which is the last recorded AoI before the departure epoch.
- B2: This block represents all entering transitions to state HP. In the category  $B_{21}$ , one of the classes related to HP arrives at an empty system. However, categories  $B_{22}$  and  $B_{23}$  symbolize the pre-

Table 1: Transition table of the SHS MC in Figure 2.

Block number	Categories	$q_l \rightarrow q'_l$	$\lambda^{(l)}$	$\mathbf{x}' = \mathbf{x}\mathbf{A}$	$\mathbf{A}_l$	$\mathbf{v}_{q_l}\mathbf{A}$
Block 1 (B1)	B <sub>11</sub>	HP $\rightarrow$ 0	$\mu$	$[x_0 \ 0]$	$\begin{bmatrix} 1 & 0 \\ 0 & 0 \end{bmatrix}$	$[v_{HP,0} \ 0]$
	B <sub>12</sub>	$m \rightarrow 0$	$\mu$	$[x_1 \ 0]$	$\begin{bmatrix} 0 & 0 \\ 1 & 0 \end{bmatrix}$	$[v_{m,1} \ 0]$
	B <sub>13</sub>	$m+i \rightarrow 0$ ( $1 \leq i \leq M-m$ )	$\mu$	$[x_0 \ 0]$	$\begin{bmatrix} 1 & 0 \\ 0 & 0 \end{bmatrix}$	$[v_{m+i,0} \ 0]$
Block 2 (B2)	B <sub>21</sub>	0 $\rightarrow$ HP	$\hat{\lambda}_m$	$[x_0 \ 0]$	$\begin{bmatrix} 1 & 0 \\ 0 & 0 \end{bmatrix}$	$[v_{0,0} \ 0]$
	B <sub>22</sub>	$m \rightarrow$ HP	$\hat{\lambda}_m p_m$	$[x_0 \ 0]$	$\begin{bmatrix} 1 & 0 \\ 0 & 0 \end{bmatrix}$	$[v_{m,0} \ 0]$
	B <sub>23</sub>	$m+i \rightarrow$ HP ( $1 \leq i \leq M-m$ )	$\hat{\lambda}_m p_{m+i}$	$[x_0 \ 0]$	$\begin{bmatrix} 1 & 0 \\ 0 & 0 \end{bmatrix}$	$[v_{m+i,0} \ 0]$
Block 3 (B3)	B <sub>31</sub>	0 $\rightarrow$ $m$	$\lambda_m$	$[x_0 \ 0]$	$\begin{bmatrix} 1 & 0 \\ 0 & 0 \end{bmatrix}$	$[v_{0,0} \ 0]$
	B <sub>32</sub>	$m \rightarrow m$	$\hat{\lambda}_m(1-p_m)$	$[x_0 \ x_1]$	$\begin{bmatrix} 1 & 0 \\ 0 & 1 \end{bmatrix}$	$[v_{m,0} \ v_{m,1}]$
	B <sub>33</sub>	$m \rightarrow m$	$\lambda_m$	$[x_0 \ 0]$	$\begin{bmatrix} 1 & 0 \\ 0 & 0 \end{bmatrix}$	$[v_{m,0} \ 0]$
	B <sub>34</sub>	$m+i \rightarrow m$ ( $1 \leq i \leq M-m$ )	$\lambda_m p_{m+i}$	$[x_0 \ 0]$	$\begin{bmatrix} 1 & 0 \\ 0 & 0 \end{bmatrix}$	$[v_{m+i,0} \ 0]$
Block 4 (B4)	B <sub>41</sub>	0 $\rightarrow$ $m+i$	$\lambda_{m+i}$	$[x_0 \ 0]$	$\begin{bmatrix} 1 & 0 \\ 0 & 0 \end{bmatrix}$	$[v_{0,0} \ 0]$
	B <sub>42</sub>	$m+i \rightarrow m+i$	$\hat{\lambda}_{m+i}(1-p_{m+i})$	$[x_0 \ 0]$	$\begin{bmatrix} 1 & 0 \\ 0 & 0 \end{bmatrix}$	$[v_{m+i,0} \ 0]$
	B <sub>43</sub>	$m+i+1 \rightarrow m+i$	$\lambda_{m+i} p_{m+i+1}$	$[x_0 \ 0]$	$\begin{bmatrix} 1 & 0 \\ 0 & 0 \end{bmatrix}$	$[v_{m+i+1,0} \ 0]$
		$\vdots$ $M \rightarrow m+i$	$\vdots$ $\lambda_{m+i} p_M$	$\vdots$ $[x_0 \ 0]$		$\vdots$ $[v_{M,0} \ 0]$

emption of class  $m$  and its lower priority classes due to the arrival of a higher priority class. This preemption is governed by the probabilistic parameter  $p_m$  for class  $m$  and  $p_{m+i}$  for the representative state  $m+i$ . Regarding the AoI resetting of the processes  $\mathbf{x}(t)$ ,  $x'_1 = 0$ , which is due to the irrelevance of the new state  $q' = \text{HP}$ . In contrast, there is no change in  $x_0(t)$  because no class  $m$  departing packet is noticed.

- B3: This block represents all possible incoming transitions into state  $m$ . In category B<sub>31</sub>, a fresh class  $m$  packet arrives at an empty server. However, Category B<sub>32</sub> refers to the case where the preemption upon class  $m$  from the higher priority classes is declined; hence, class  $m$  continues its service normally. Categories B<sub>33</sub> and B<sub>34</sub> represent the preemption occurs due to the arrival of a fresh packet of class  $m$ . More specifically, B<sub>33</sub> denotes the self-preemption, whereas B<sub>34</sub> considers the preemptions over the lower priority classes. All categories related to this block yield no change in the AoI process  $x_0(t)$ . However, in categories

B<sub>31</sub>, B<sub>33</sub> and B<sub>34</sub>,  $x'_1 = 0$  since a fresh relevant packet of class  $m$  starts the service. This is in contrast with B<sub>33</sub>, where the already existing packet of class  $m$  continues its service without interruption; hence,  $x'_1 = x_1$ .

- B4: This block lists all incoming transition into the representative state  $m+i$  ( $1 \leq i \leq M-m$ ). In the first category, the server is empty before being occupied with a packet of class  $m+i$ ,  $1 \leq i \leq M-m$ . In category B<sub>42</sub>, the interruptions over class  $m+i$  from the higher priority classes are declined. However, category B<sub>43</sub> lists all cases where the lower priority classes of class  $m+i$  are preempted due to an arrival of class  $m+i$ . In all these categories,  $x_0(t)$  is unchanged since there is no departure of class  $m$ . However,  $x_1(t)$  is reset to 0 due to the irrelevance of the new state  $q' = m+i$ .

The AoI analysis begins with finding the stationary state probabilities  $\bar{\pi} = [\bar{\pi}_0, \bar{\pi}_{HP}, \bar{\pi}_m, \bar{\pi}_{m+i}]$ . Applying equation (4) at each state  $q \in \mathcal{Q}$ , a system of linear equations can be formulated as follows:

at state  $q = \{0\}$ :

$$\pi_0(\lambda_{\text{total}}) = \mu \sum_{q \in Q \setminus \{0\}} \pi_q, \quad (11)$$

at state  $q = \{\text{HP}\}$ :

$$\pi_{\text{HP}}(\mu) = \hat{\lambda}_m(\pi_0 + \sum_{j=m}^M \pi_j p_j), \quad (12)$$

at state  $q = \{m\}$ :

$$\pi_m(\mu + \hat{\lambda}_m p_m) = \lambda_m(\pi_0 + \sum_{j=m+1}^M \pi_j p_j), \quad (13)$$

at state  $q = \{m+i\}$  for  $1 \leq i \leq M-m$ :

$$\pi_{m+i}(\mu + \hat{\lambda}_{m+i} p_{m+i}) = \lambda_{m+i}(\pi_0 + \sum_{j=m+i+1}^M \pi_j p_j). \quad (14)$$

This system of linear equations is to be solved with the normalization equation described at (5).

After finding the probability vector  $\bar{\pi}$ , the correlation vector  $\bar{v}$  for all states  $q \in Q$  can be evaluated using equation (7). However, some of these correlations will be vanished intuitively; more specifically,  $\bar{v}_{0,1} = \bar{v}_{\text{HP},1} = 0$ , along with  $\bar{v}_{m+i,1} = 0$  ( $1 \leq i \leq M-m$ ). This is because all these correlation values irrelevant to class  $m$ . In the following, equation (7) is applied at each state  $q \in Q$  according to the information tabulated in Table 1:

at state  $q = \{0\}$ :

$$[\bar{v}_{0,0} \ \bar{v}_{0,1}] (\lambda_{\text{total}}) = [\pi_0 \ 0] + \mu [\bar{v}_m \ 0] + \mu \sum_{q \in Q \setminus \{0,m\}} [\bar{v}_{q,0} \ 0], \quad (15)$$

at state  $q = \{\text{HP}\}$ :

$$[\bar{v}_{\text{HP},0} \ \bar{v}_{\text{HP},1}] (\mu) = [\pi_{\text{HP}} \ 0] + \hat{\lambda}_m([\bar{v}_{0,0} \ 0] + \sum_{j=m}^M [\bar{v}_{j,0} \ 0] p_j), \quad (16)$$

at state  $q = \{m\}$ :

$$\begin{aligned} [\bar{v}_{m,0} \ \bar{v}_{m,1}] (\mu + \hat{\lambda}_m + \lambda_m) &= [\pi_m \ \pi_m] \\ + \lambda_m([\bar{v}_{0,0} \ 0] + [\bar{v}_{m,0} \ 0] + \sum_{j=m+1}^M [\bar{v}_{j,0} \ 0] p_j) \\ + \hat{\lambda}_m(1 - p_m)[\bar{v}_{m,0} \ \bar{v}_{m,1}], \end{aligned} \quad (17)$$

at state  $q = \{m+i\}$  for  $1 \leq i \leq M-m$ :

$$\begin{aligned} [\bar{v}_{m+i,0} \ \bar{v}_{m+i,1}] (\mu + \hat{\lambda}_{m+i}) &= [\pi_{m+i} \ 0] \\ + \lambda_{m+i}([\bar{v}_{0,0} \ 0] + \sum_{j=m+i+1}^M [\bar{v}_{j,0} \ 0] p_j) \\ + \hat{\lambda}_{m+i}(1 - p_{m+i})[\bar{v}_{m+i,0} \ 0]. \end{aligned} \quad (18)$$

After solving the above system of vector equations, the correlation vector  $\bar{v}$  is reached. Hence, the average AoI of class  $m$  ( $E[\Delta_m]$ ) can be evaluated using equation (9) as follows:

$$E[\Delta_m] = \bar{v}_{0,0} + \bar{v}_{\text{HP},0} + \bar{v}_{m,0} + \sum_{i=1}^{M-m} \bar{v}_{m+i,0} \quad (19)$$

It should be noted that the algorithm adopted to find  $E[\Delta_m]$  can be deployed similarly for the other priority classes.

## 4 NUMERICAL RESULTS

In this section, the analytical framework will be numerically investigated. Throughout this numerical study, three prioritized status update streams are considered. In addition, unless otherwise indicated, the homogeneous arrival process is assumed between all classes, where  $\lambda_1 = \lambda_2 = \lambda_3 = \frac{1}{3} \lambda_{\text{total}}$  and  $\mu = 1$ . Moreover, the average service rate is identical for all classes with  $\mu = 1$ .

The numerical study will be initiated, in section 4.1, by validating the analytical framework through simulation. After that, the proposed model will be compared with the PP model (Kaul and Yates, 2018) and the SP mentioned in (Farazi et al., 2019) taking into consideration the priority setting. This comparative study is established through three different approaches, by which the probabilistic hybrid parameters ( $p_2$  and  $p_3$ ) can be generated.

### 4.1 Analytical Model Validation

In this section, the analytical model will be verified under a simulation framework similar to the analytical one using MATLAB R2015a. The simulation time is to be lengthy enough ( $10^5$  time units) to capture the steady state results. Moreover, The simulation environment was built through a workstation with the following specifications: Intel(R) Xeon(R) Gold 6230R CPU, 2.10 GHz (2 processors); 128 GB RAM; and 64 bit Windows 10 pro operating system.

In this study, two different cases of the probabilistic hybrid parameters are experimented,  $p_2 = p_3 = \frac{1}{2}$  and  $p_2 = p_3 = \frac{2}{3}$ , as shown in Figure 3a and Figure 3b, respectively. It is demonstrated that the simulation results conform with the analytical results with maximum percentage errors of 2.437 % and 3.6952 % in the cases of Figure 3a and Figure 3b, respectively.

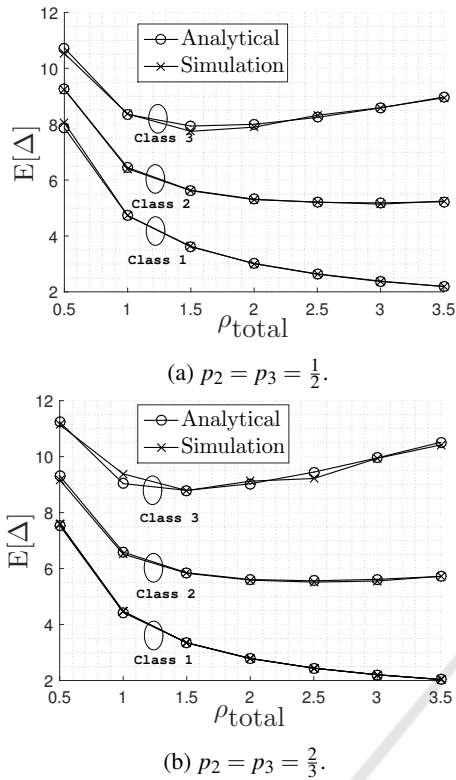


Figure 3: Comparison between the analytical and simulation results.

## 4.2 Comparison with the Classical Approaches

In the subsequent studies, the probabilistic hybrid approach will be compared with the PP and SP models. In this study, three different methods will be presented to determine how to set the probabilistic hybrid parameters  $p_2$ ,  $p_3$ : fixed assignment approach, optimization-based approach, and interruption-based approach.

### 4.2.1 Fixed Assignment Probabilistic (FAP) Approach

In this approach, the probabilistic hybrid parameters  $p_2$ ,  $p_3$  are considered as decision-making parameters to be set irrespective of any traffic and system conditions. Figure 4 elaborates the comparison between the proposed hybrid approach and the classical ones under two different setting of the hybrid parameters,  $p_2 = p_3 = 0.3$  and  $p_2 = p_3 = 0.7$ . The observations on this figure are analyzed in the following notes:

- In comparison with the PP model, the SP model yields an improvement for the lower priority classes at the cost of a dramatic degradation in class 1 performance. On the other hand, the pro-

posed hybrid approach significantly reduces class 1 degradation while keeping an acceptable improvement gain for the lower priority classes.

- As the probability of preemption increases, the probabilistic hybrid model approaches the PP model, which is in favour of the higher priority class at the expense of the lower priority ones.

For further elaboration, Figure 5 presents the improvement/degradation percentage in the average AoI of each class with respect to the PP mode at three different loading conditions. This percentages are to be evaluated as  $\frac{E[\Delta_m|PP] - E[\Delta_m|scheme]}{E[\Delta_m|PP]} \times 100$ , where  $E[\Delta_m|scheme]$  and  $E[\Delta_m|PP]$  are the average AoI under the operating scheme and the PP model, respectively. As shown in Figure 5a, the significance of the proposed model is manifested vividly at the higher traffic loading conditions. In such case, the performance gain of the lower priority classes increases; meanwhile, the degradation experienced by class 1 is improved gradually. This is in contrast with the SP model as shown in Figure 5b, where the degradation occurs for class 1 increases as the traffic loading becomes worse.

In conclusion, the proposed model not only gives a compromise solution compared with the PP and SP model, but it also seems to be much more efficient at the worse traffic loading conditions. From another perspective, in case of using the FAP, it is preferable to control the offered load to be as high as possible.

### 4.2.2 Optimization-based Probabilistic (OBP) Approach

In this approach, another method is adopted to determine the setting of the probabilistic hybrid parameters ( $p_2$ ,  $p_3$ ). In such approach, these parameters will be the decision variables resulting from a constrained optimization problem of a cost function  $C_{\alpha_1, \alpha_2, \alpha_3}$ , which is represented as the weighted sum of the average AoI of each prioritized class. This cost function signifies the overall satisfaction of the whole network.

The optimization problem is formulated as follows:

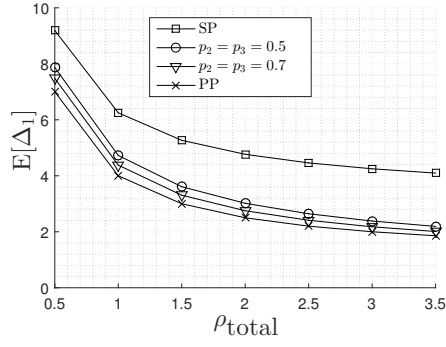
$$\begin{aligned} \min_{p_2, p_3} C_{\alpha_1, \alpha_2, \alpha_3} &= \alpha_1 \times E[\Delta_1] + \alpha_2 \times E[\Delta_2] \\ &+ \alpha_3 \times E[\Delta_3], \\ 0 &\leq \alpha_1, \alpha_2, \alpha_3 \leq 1 \end{aligned} \quad (20)$$

subject to

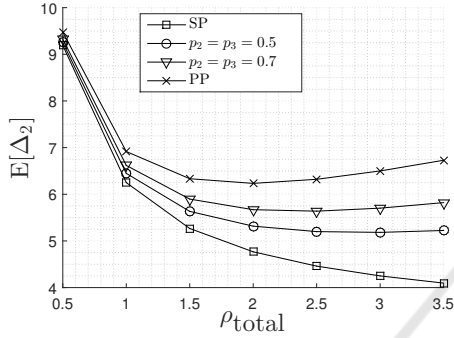
$$\frac{E[\Delta_1|scheme] - E[\Delta_1|PP]}{E[\Delta_1|PP]} \times 100 \leq R \%,$$

where  $E[\Delta_1|scheme]$  and  $E[\Delta_1|PP]$  are as mentioned before in section 4.2.1.

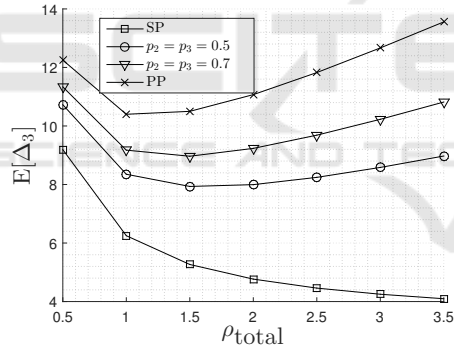
The cost function parameters ( $\alpha_1, \alpha_2, \alpha_3$ ) are chosen to reflect the distinction in the importance of each



(a) Class 1.



(b) Class 2.



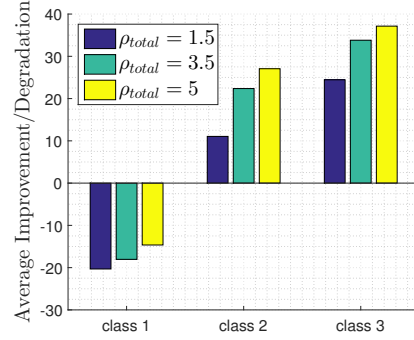
(c) Class 3.

Figure 4: Comparison between the proposed hybrid discipline, along with PP and SP approaches for each class.

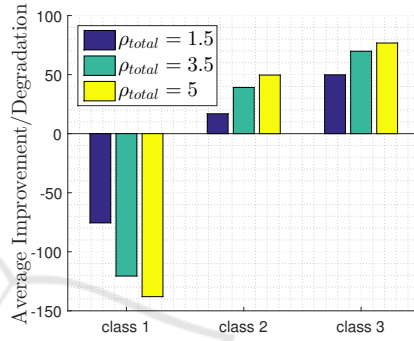
corresponding class compared with the others. For instance, in case of  $\alpha_1 = \alpha_2 = \alpha_3$ , the sources will be with equally importance. However, the setting  $\alpha_1 > \alpha_2 > \alpha_3$  refers to the case of prioritized network. From another perspective. As regards to the adopted constraint, it represents an upper bound limit of the degradation percentage incurred by class 1 due to the use of the hybrid mode instead of its most preferable approach (PP model).

To solve this constrained optimization problem, the brute-force approach is employed with a resolution of 0.1 for each probabilistic parameter  $p_m$ .

Table 2 presents the resulting optimal probabilistic



(a) The proposed model.



(b) Self-preemption model (SP).

 Figure 5: The Improvement/Degradation in the average AoI with respect to the PP mode at  $\rho_{total} = 1.5$ ,  $\rho_{total} = 3.5$  and  $\rho_{total} = 5$ .

hybrid probabilities ( $p_2^*$ ,  $p_3^*$ ) over the span of  $\rho_{total} = [0, 0.5]$  for the three different cases of the cost function:  $C_{1,1,1}$ ,  $C_{1,\frac{1}{2},\frac{1}{4}}$ , and  $C_{1,\frac{1}{4},\frac{1}{8}}$ . As demonstrated in the table, the case of the PP ( $p_2 = 1$  and  $p_3 = 1$ ) is not always the optimal choice for the network to fulfill the network level of satisfaction represented in the cost function  $C_{\alpha_1,\alpha_2,\alpha_3}$ , while the proposed hybrid discipline, by its controlling parameters, can be adjusted for such purpose.

For further illustration, in Figure 6, the cost function  $C_{\alpha_1,\alpha_2,\alpha_3}$  with different weight parameters is examined under three different approaches: PP, SP, and the optimization-based approach (OBP). In this study, the homogeneous traffic loading is also assumed. Generally speaking, the cost function metric, as a weighted sum, will be intuitively more sensitive to the performance of the class having the highest weight parameter. Accordingly, we can derive the following investigations:

- In Figure 6a, the equal-weight cost function  $C_{1,1,1}$  is minimized in the SP model and worsened in the PP model, which is outperformed by the OBP model. This is because  $C_{1,1,1}$  is equally sensitive to the performance gain yielded for any of the

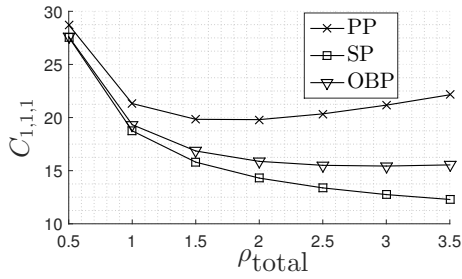
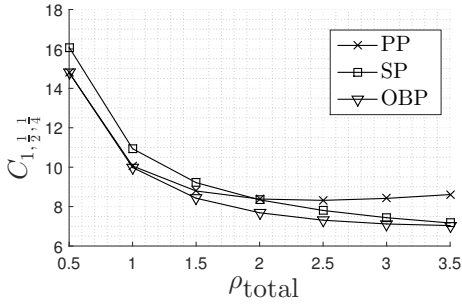
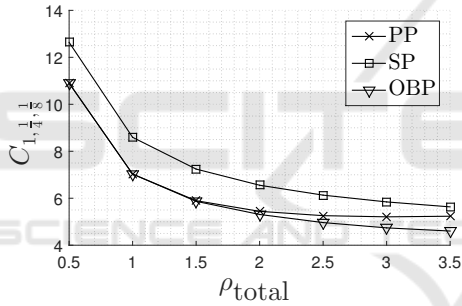

 (a)  $\alpha_1 = \alpha_2 = \alpha_3 = 1$ .

 (b)  $\alpha_1 = 1, \alpha_2 = \frac{1}{2}, \alpha_3 = \frac{1}{4}$ .

 (c)  $\alpha_1 = 1, \alpha_2 = \frac{1}{4}, \alpha_3 = \frac{1}{8}$ .

 Figure 6: The cost function  $C_{\alpha_1, \alpha_2, \alpha_3}$  under three different schemes (PP, SP, and OBP) for three cases of the cost function parameters.

priority classes. In this regard, as shown in Figure 4, the performance gain achieved by the SP model for class 2,3 outperforms the improvement yielded from the other models.

- In Figures 6b and 6c, the proposed OBP model represents the most optimal choice. In such case, the sensitivity of the cost functions  $C_{1, \frac{1}{2}, \frac{1}{4}}$  and  $C_{1, \frac{1}{4}, \frac{1}{8}}$  becomes in line with the priority order of the classes. Therefore, the compromise performance achieved by OBP overtakes the other models due to its contribution to improve class 2,3 with respect to the PP model in addition to enhancing class 1 performance with respect to SP model.

Based on the foregoing investigations, the OBP is the

most optimal choice to enhance the overall performance satisfaction of the prioritized network.

 Table 2: The probabilistic hybrid parameters under different cases of  $C_{\alpha_1, \alpha_2, \alpha_3}$ .

$\rho_{total}$	$C_{1,1,1}$		$C_{1, \frac{1}{2}, \frac{1}{4}}$		$C_{1, \frac{1}{4}, \frac{1}{8}}$	
	$p_2^*$	$p_3^*$	$p_2^*$	$p_3^*$	$p_2^*$	$p_3^*$
0.5	0.4	0.2	1	1	1	1
1	0.7	0.3	0.7	0.7	1	1
1.5	0.7	0.3	0.6	0.5	1	0.7
2	0.7	0.3	0.6	0.4	0.7	0.6
2.5	0.7	0.3	0.6	0.4	0.6	0.4
3	0.7	0.3	0.6	0.4	0.6	0.4
3.5	0.7	0.3	0.6	0.4	0.6	0.4

### 4.2.3 Interruption-based Probabilistic Approach (IBP)

In this approach, the working probabilistic hybrid Parameters ( $p_2, p_3$ ) are generated based on the average number of preemptions experienced by each class. However, the self-preemptions will be excluded from this measure. This is due to the benefit behind the self-preemptions in enhancing the information freshness of each class.

In our setting, the following is the formulation of the average number of preemptions of class  $m$  caused by the higher priority classes  $k$  ( $0 \leq k \leq m-1$ ) per unit time:

$$E[N^{(m)}] = \left( \sum_{k=1}^{m-1} \lambda_k \times p_m \right) \times r_m, \quad (21)$$

where  $r_m$  is the corresponding probability that class  $m$  is being served.

After formulating  $E[N^{(m)}]$ , it will be deployed to generate the probabilistic hybrid parameters ( $p_m$ ) at each traffic loading condition. This generation is performed using a decaying exponential function of parameter  $a_m$  as follows:

$$p_m = e^{-(a_m \times E[N^{(m)}|pp])}, \quad 2 \leq m \leq M, \quad a_m \geq 0, \quad (22)$$

where  $E[N^{(m)}|PP]$  is the average number of preemptions of class  $m$  while applying the PP model, which is the worst case of preemptions that class  $m$  can experience. Moreover, the parameter  $a_m$  is used to control the decaying rate of the exponential function. Accordingly, if the traffic loading conditions becomes worse, the exponential decaying function makes  $p_m$  be decreased to counter the potential increase in the number of preemptions. This in turn enhances the AoI performance of the lower priority classes. Moreover, it should be noted that the PP model corresponds to  $a_m = 0$  for ( $1 \leq m \leq M$ ), while the SP model can be reached by setting  $a_m = \infty$  for ( $1 \leq m \leq M$ ).

To visualize the above result, the effect of the interruption-based approach can be emerged using what is called the admissible control regions. These regions demonstrate the maximum offered load that the network can tolerate without violating some system constraints.

In Figure 7, the admissible region for class 2 is depicted to highlight the maximum traffic loading of class 2 over the span of class 1's offered load, while levelling off  $\rho_3 = 1$ . This admission region is restricted by two constraints:  $E[\Delta_1] < 2$  and  $E[\Delta_3] < 20$ . These constraints are set on class 1 and 3, particularly, because class 1 is the most AoI sensitive one while class 3 is the highly interrupted traffic.

As shown in Figure 7, the following investigations can be derived:

- In the PP model, the admission region becomes more dense at lower class 1's traffic intensities, while being shrunk at the higher intensities. This is expected because the PP model causes a dramatic degradation for class 3; therefore, the AoI constraint ( $E[\Delta_3] < 20$ ) becomes more vulnerable to be violated at the higher zone of  $\rho_1$ . This is in contrast with the SP model, where a higher degradation occurs for class 1; hence, the AoI constraint ( $E[\Delta_1] < 2$ ) is more prone to be violated at lower range of  $\rho_1$ .
- Regarding the probabilistic hybrid approach, it is clear that as  $a_2$  and  $a_3$  increase, the admissible region shrinks at the lower span of  $\rho_1$ , while widening at the higher values of this span. This is because the more  $a_2$  and  $a_3$  increase, the more the system approaches the SP model. Hence, for each setting of  $a_m$ , it is impossible to widen the admissible region over the whole span of  $\rho_1$ .

To tackle the above mentioned problem, it is proposed that  $a_2, a_3$  can be adjusted to increase in line with the increase of  $\rho_1$ . In such case, the system will be self-adapted with the expected traffic conditions. In Figure 8, the self-adapted IBP approach is experimented, where  $a_2, a_3$  increase linearly from 0 to 10 over the span of  $\rho_1 = [0.5, 3.5]$ . As shown in the figure, the admission region is enhanced over the whole span of  $\rho_1$ .

## 5 CONCLUSIONS

In this paper, the probabilistic hybrid service discipline is proposed to be deployed in a network with prioritized traffic. In the proposed discipline, the preemptions towards a certain class, resulting from the higher priority ones, are admitted with a certain prob-

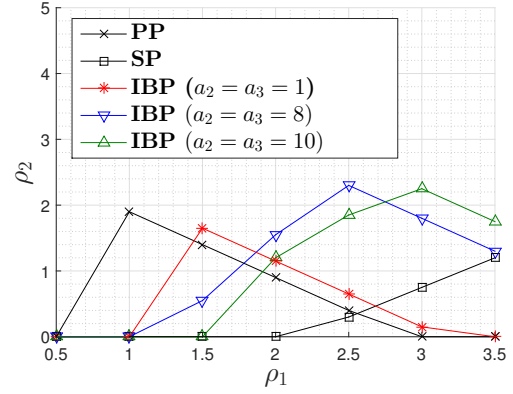


Figure 7: Admissible region for class 2 under three different schemes: PP, SP and IBP approach.

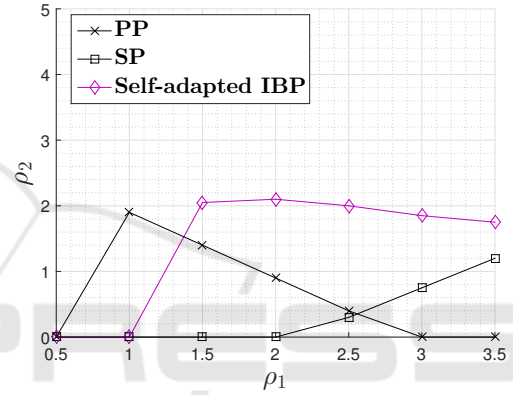


Figure 8: Admissible region for class 2 under three different schemes: PP, SP and self-adapted IBP approach.

ability. However, the self preemptions are always permitted. The SHS approach is used to analyze the average AoI for each prioritized class. To corroborate the theoretical framework, a numerical study of a network of three prioritized classes is provided. Based on this setting, the performance of the proposed hybrid discipline is compared with the conventional disciplines, PP and SP. As these classical policies result in an improvement for some specific class with a dramatic degradation for the others, the proposed hybrid discipline resolves this drawback by reducing the downside effect of the adversely affected classes. Furthermore, the proposed hybrid discipline renders some controlling parameters by which the system performance can be adjusted. In the FAP, it is preferable to control the offered load to be as high as possible to guarantee marginal degradation for class 1 with an increasing improvements for class 2 and 3. On the other hand, in the OBP approach, It was found that the probabilistic hybrid approach becomes the optimal choice to optimize a cost function, which represents the whole network satisfaction. Furthermore, a

much simpler method is proposed (IBP) to attribute the generation of the probabilistic parameters to the average number of interruptions experienced under the working traffic loading conditions. According to this setting, the superiority of the proposed model is manifested in widening the feasible region of the acceptable offered load without violating some AoI constraints.

As a future work, the presented study can be extended by experimenting another discretionary rule for the hybrid discipline rather than the probabilistic one. Moreover, the analytical study can be also extended by considering general arrival and service stochastic processes.

## ACKNOWLEDGEMENTS

This research work is sponsored by the Egyptian Ministry of Higher Education (MoHE) grant in the scope of the Egypt-Japan University of Science and Technology (E-JUST).

## REFERENCES

- Abbas, Q., Hassan, S. A., Pervaiz, H., and Ni, Q. (2021). A markovian model for the analysis of age of information in IoT networks. *IEEE Wireless Communications Letters*, 10(7):1596–1600.
- Costa, M., Codreanu, M., and Ephremides, A. (2016). On the age of information in status update systems with packet management. *IEEE Transactions on Information Theory*, 62(4):1897–1910.
- Fahim, T. E., Zakariya, A. Y., and Rabia, S. I. (2018). A novel hybrid priority discipline for multi-class secondary users in cognitive radio networks. *Simulation Modelling Practice and Theory*, 84:69–82.
- Farazi, S., Klein, A. G., and Brown, D. R. (2019). Average age of information in multi-source self-preemptive status update systems with packet delivery errors. In *53rd Asilomar Conference on Signals, Systems, and Computers*, Pacific Grove, CA, USA, pages 396–400. IEEE.
- Hespanha, J. P. (2006). Modelling and analysis of stochastic hybrid systems. *IEE Proceedings-Control Theory and Applications*, 153(5):520–535.
- Kaul, S., Yates, R., and Gruteser, M. (2012a). Real-time status: How often should one update? In *Proceedings IEEE INFOCOM*, Orlando, FL, USA, pages 2731–2735. IEEE.
- Kaul, S. K. and Yates, R. D. (2018). Age of information: Updates with priority. In *IEEE International Symposium on Information Theory (ISIT)*, Vail, CO, USA, pages 2644–2648. IEEE.
- Kaul, S. K., Yates, R. D., and Gruteser, M. (2012b). Status updates through queues. In *46th Annual Conference on Information Sciences and Systems (CISS)*, Princeton, NJ, USA, pages 1–6. IEEE.
- Kim, K. (2012). T-preemptive priority queue and its application to the analysis of an opportunistic spectrum access in cognitive radio networks. *Computers & Operations Research*, 39(7):1394–1401.
- Maatouk, A., Assaad, M., and Ephremides, A. (2019). Age of information with prioritized streams: When to buffer preempted packets? In *IEEE International Symposium on Information Theory (ISIT)*, Paris, France, pages 325–329. IEEE.
- Mishra, S., Mishra, B. K., Tripathy, H. K., and Dutta, A. (2020). Analysis of the role and scope of big data analytics with iot in health care domain. In *Handbook of data science approaches for biomedical engineering*, pages 1–23. Elsevier.
- Najm, E., Nasser, R., and Telatar, E. (2019). Content based status updates. *IEEE Transactions on Information Theory*, 66(6):3846–3863.
- Sun, Y., Uysal-Biyikoglu, E., Yates, R. D., Koksal, C. E., and Shroff, N. B. (2017). Update or wait: How to keep your data fresh. *IEEE Transactions on Information Theory*, 63(11):7492–7508.
- Talak, R., Karaman, S., and Modiano, E. (2016). Speed limits in autonomous vehicular networks due to communication constraints. In *IEEE 55th Conference on Decision and Control (CDC)*, Las Vegas, NV, USA, pages 4998–5003. IEEE.
- Teel, A. R., Subbaraman, A., and Sferlazza, A. (2014). Stability analysis for stochastic hybrid systems: A survey. *Automatica*, 50(10):2435–2456.
- Xu, J. and Gautam, N. (2020). Peak age of information in priority queuing systems. *IEEE Transactions on Information Theory*, 67(1):373–390.
- Yates, R. D. and Kaul, S. K. (2018). The age of information: Real-time status updating by multiple sources. *IEEE Transactions on Information Theory*, 65(3):1807–1827.
- Yates, R. D., Sun, Y., Brown, D. R., Kaul, S. K., Modiano, E., and Ulukus, S. (2021). Age of information: An introduction and survey. *IEEE Journal on Selected Areas in Communications*, 39(5):1183–1210.